

Supporting Information

An injectable and self-healing hydrogel with antibacterial and angiogenic properties for diabetic wound healing

Xuexia Liu,^{a, b, c} Sijie Zhou,^b Biying Cai,^b Yanan Wang,^{b, d} Dan Deng,^{a, b} and Xiaolei Wang^{a, b*}

a. College of Chemistry, Nanchang University, Nanchang, Jiangxi, 330088 (P.R. China)

b. The National Engineering Research Center for Bioengineering Drugs and the Technologies, Institute of Translational Medicine, Nanchang University, Nanchang, Jiangxi, 330088 (P.R. China)

c. College of Chemistry and Chemical Engineering, Jingtangshan University, Ji'an Jiangxi, 343009 (P.R. China)

d. Affiliated Eye Hospital of Nanchang University, Nanchang University, Nanchang, Jiangxi, 330006 (P.R. China)

*Corresponding author.

* E-mail: wangxiaolei@ncu.edu.cn Tel: 0791-83827416.

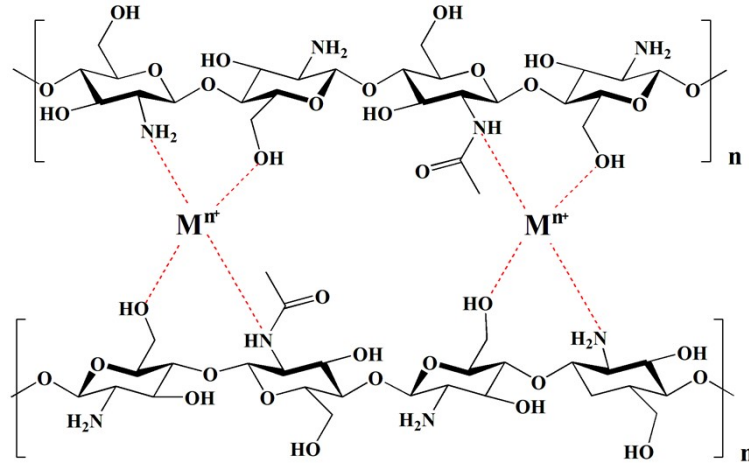


Fig. S1. The mechanism of the complexation between CS and the metal ions.

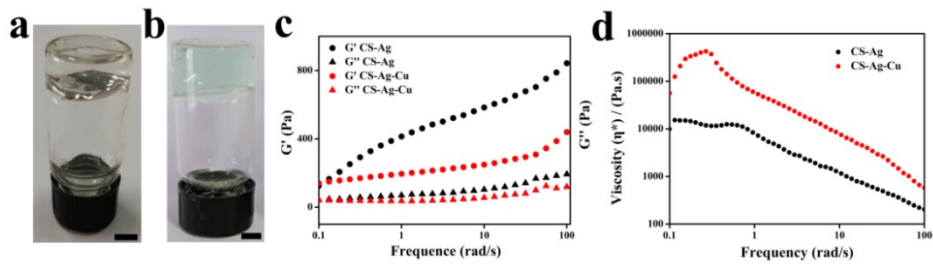


Fig. S2. (a, b) Digital photographs of CS-Ag hydrogel (a) and CS-Ag-Cu hydrogel (b) (Scale bar = 0.5 cm). (c) Dynamic frequency sweep of the hydrogels at 2% strain. (d) Viscosity of the hydrogels with a shear rate ranging from 0.1 to 100 rad/s at 25 °C.

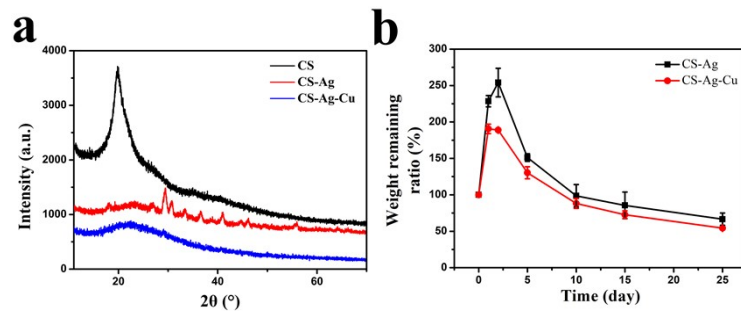


Fig. S3. (a) XRD patterns of the CS powder, CS-Ag hydrogel and CS-Ag-Cu hydrogel. (b) Degradation behavior of CS-Ag hydrogel and CS-Ag-Cu hydrogel in PBS solution at 37 °C for 25 days. Data are expressed as mean \pm SD. ($n = 3$).

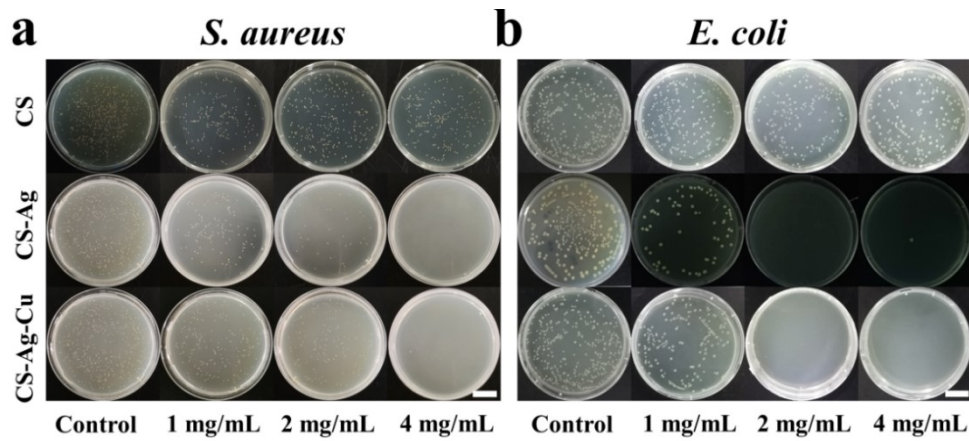


Fig. S4. (a, b) Digital photographs of agar plates of *S. aureus* (a) and *E. coli* (b) colonies of each group after incubating for 6 h (Scale bar = 2 cm).

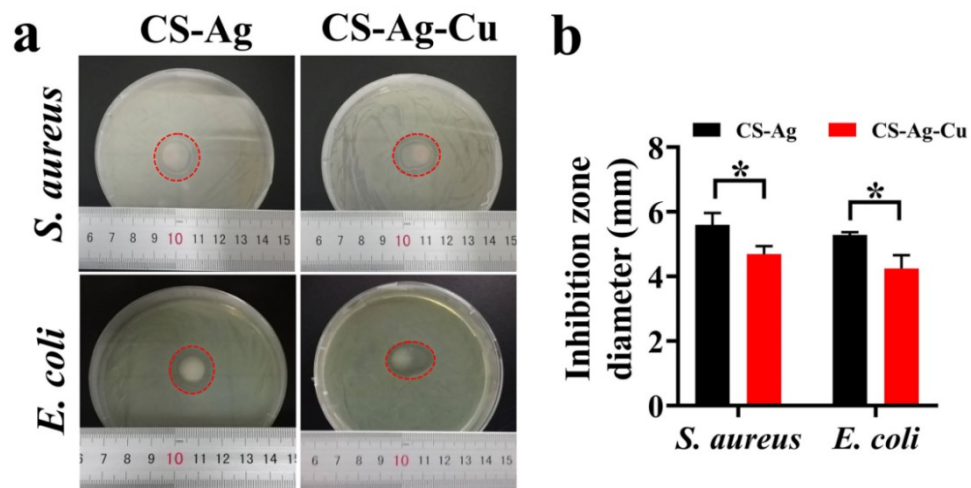


Fig. S5. (a) Antibacterial activities of hydrogels against *S. aureus* and *E. coli* with agar diffusion test at 24 h. (b) Inhibition zone diameters in CS-Ag and CS-Ag-Cu groups. Data are expressed as mean \pm SD. ($n = 3$). * $p < 0.05$, ** $p < 0.01$, *** $p < 0.001$.

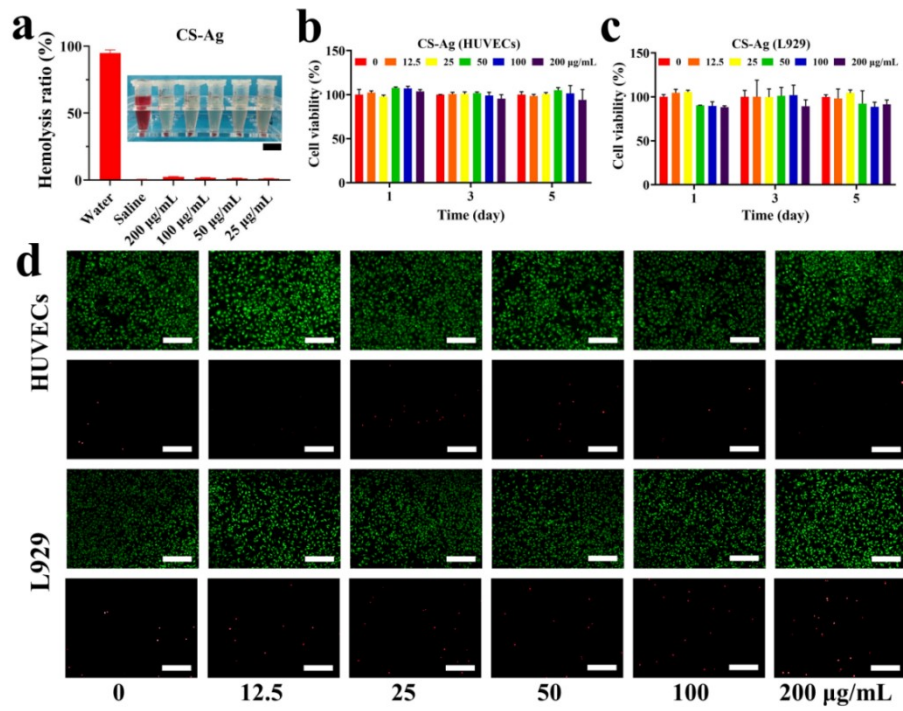


Fig. S6. Biocompatibility evaluation of the CS-Ag hydrogel *in vitro*. (a) Hemolytic ratio of the CS-Ag hydrogel, the inset is the corresponding picture of RBC hemolysis (Scale bar = 1 cm). (b, c) Cell viability of HUVECs (b) and L929 (c) co-cultured with CS-Ag hydrogel extracts for 1, 3, 5 days, respectively. (d) Live/dead staining fluorescent images of HUVECs and L929 after treatment with CS-Ag hydrogel (Scale bar = 200 µm). Data are expressed as mean ± SD. ($n = 3$).

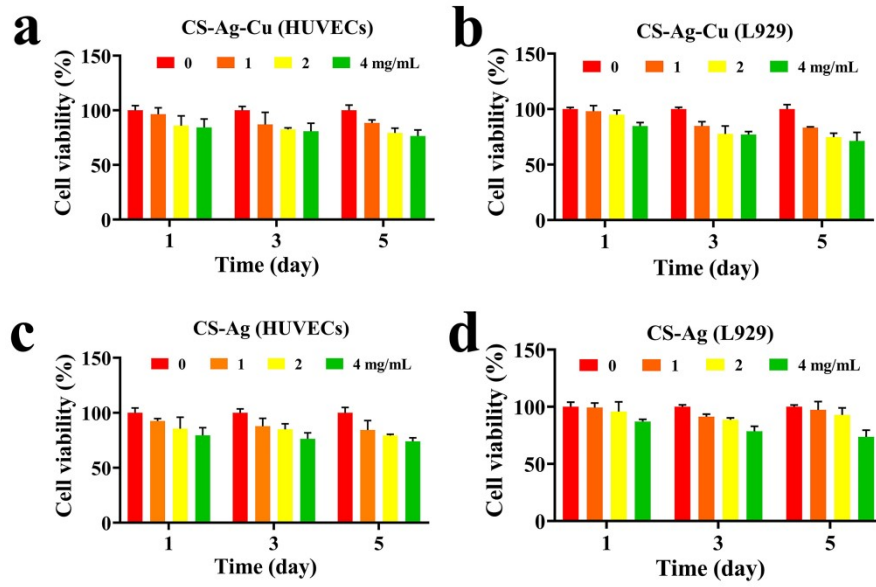


Fig. S7. (a, b) Cell viability of HUVECs (a) and L929 (b) co-cultured with CS-Ag-Cu hydrogel extracts (1, 2, 4 mg/mL) for 1, 3, 5 days, respectively. (c, d) Cell viability of HUVECs (c) and L929 (d) co-cultured with CS-Ag hydrogel extracts (1, 2, 4 mg/mL) for 1, 3, 5 days, respectively. Data are expressed as mean \pm SD. ($n = 3$).

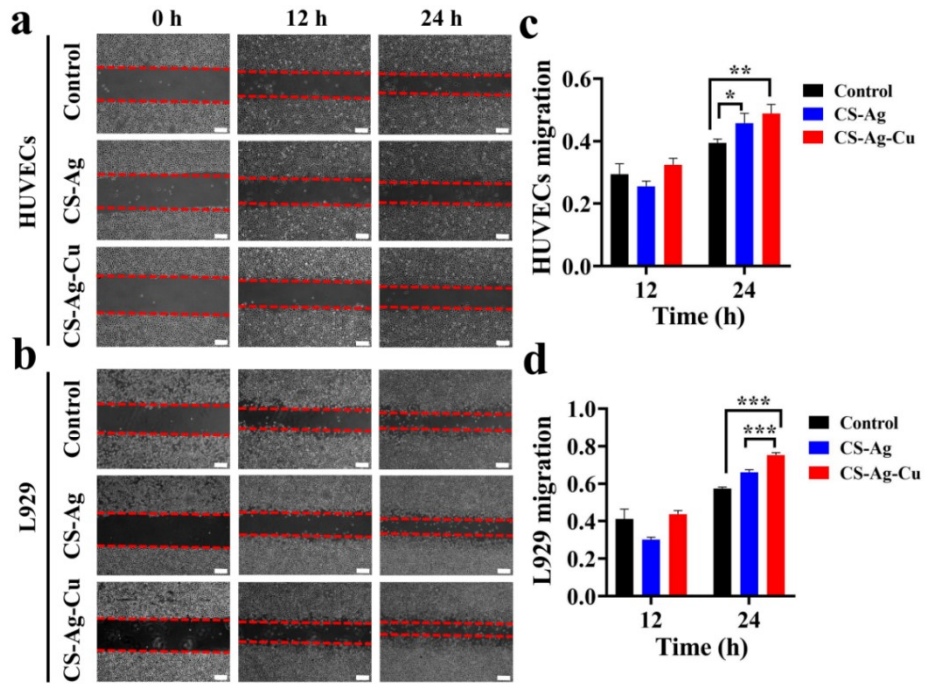


Fig. S8. (a, b) Scratch assay digital images of HUVECs (a) and L929 (b) after different treatments (Scale bar = 200 μm). (c, d) Quantification of HUVECs (c) and L929 (d) migration. Data are expressed as mean \pm SD. ($n = 3$). * $p < 0.05$, ** $p < 0.01$, *** $p < 0.001$.

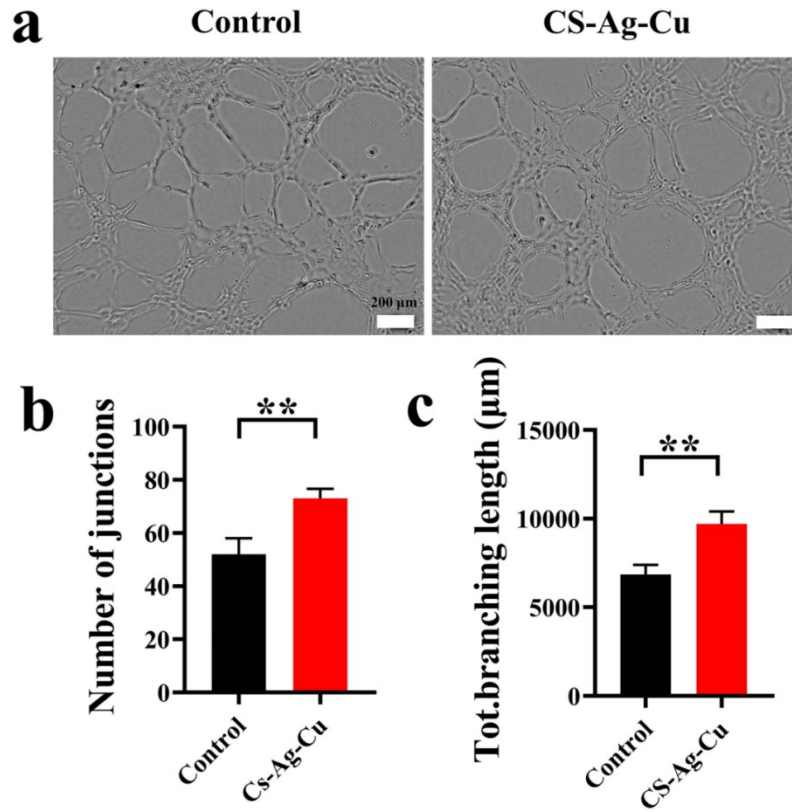


Fig. S9. (a) Digital images of HUVECs treated with PBS, CS-Ag-Cu hydrogel for 6 h. (b, c) Quantification of junctions (b) and total branching length (c) of digital images of HUVECs. Data are expressed as mean \pm SD. ($n = 3$). * $p < 0.05$, ** $p < 0.01$, *** $p < 0.001$.

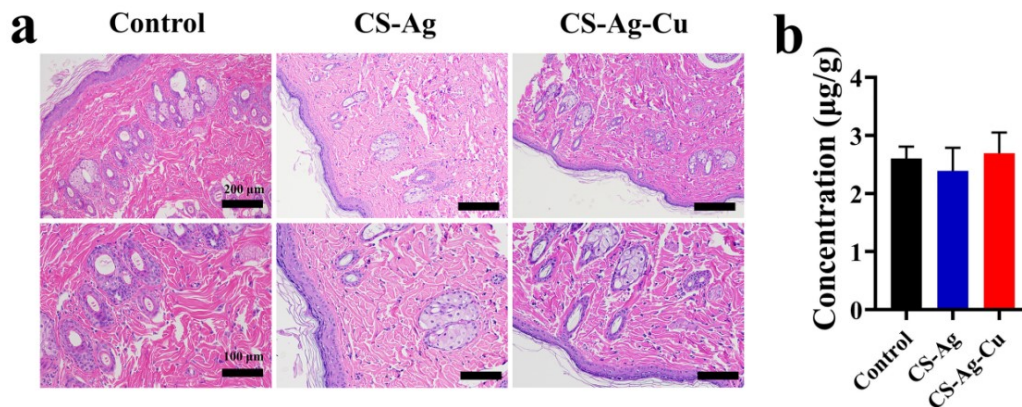


Fig. S10. (a) H&E staining of the tissues around the injection sites from different groups after 14 days of treatment. (b) Quantification of Cu^{2+} content in tissues. Data are expressed as mean \pm SD. ($n = 3$). * $p < 0.05$, ** $p < 0.01$, *** $p < 0.001$.

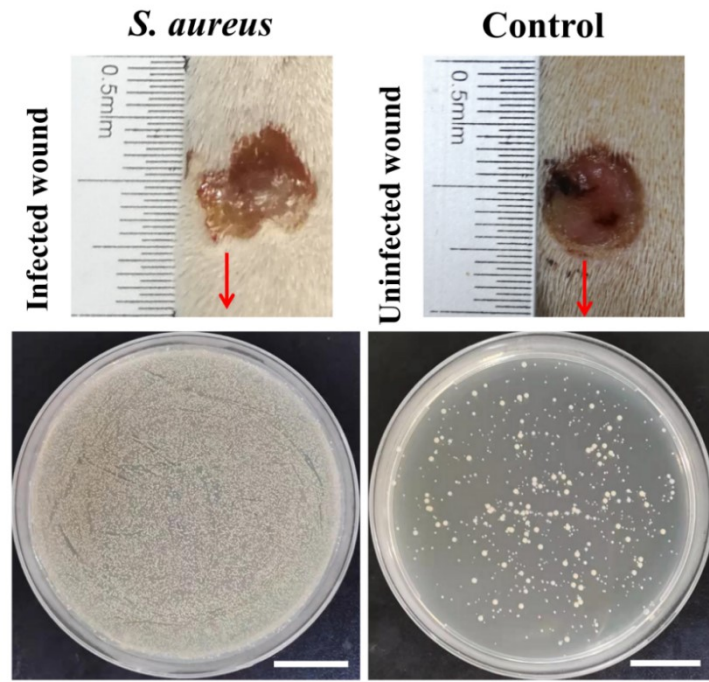


Fig. S11. Digital photographs of *S. aureus* infected wound and uninfected wound, and the corresponding images of bacterial colony plates (Scale bar = 2 cm).

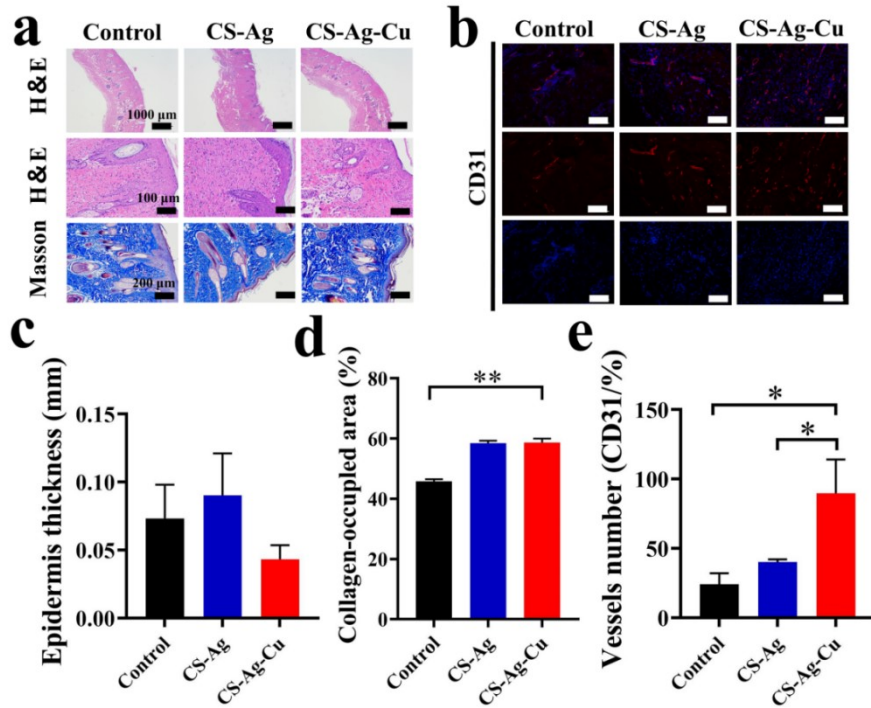


Fig. S12. (a) Micrographs of H&E and Masson staining tissue slices from different groups after 14 days of treatment. (b) Immunofluorescence images of the expression of CD31 (red) and DAPI (blue) in skin wound tissues on day 14 (Scale bar = 100 μ m). (c-e) Quantitative analysis of epidermis thickness (c), collagen deposition (d), and vessels number (e) for each group. Data are expressed as mean \pm SD. ($n = 3$). * $p < 0.05$, ** $p < 0.01$, *** $p < 0.001$.

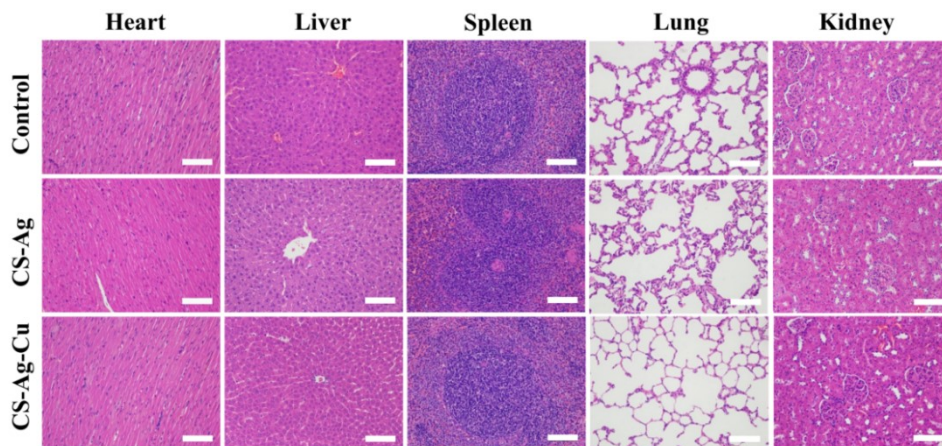


Fig. S13. H&E staining images of heart, liver, spleen, lung and kidney in different groups of rats, respectively (Scale bar = 100 μ m).

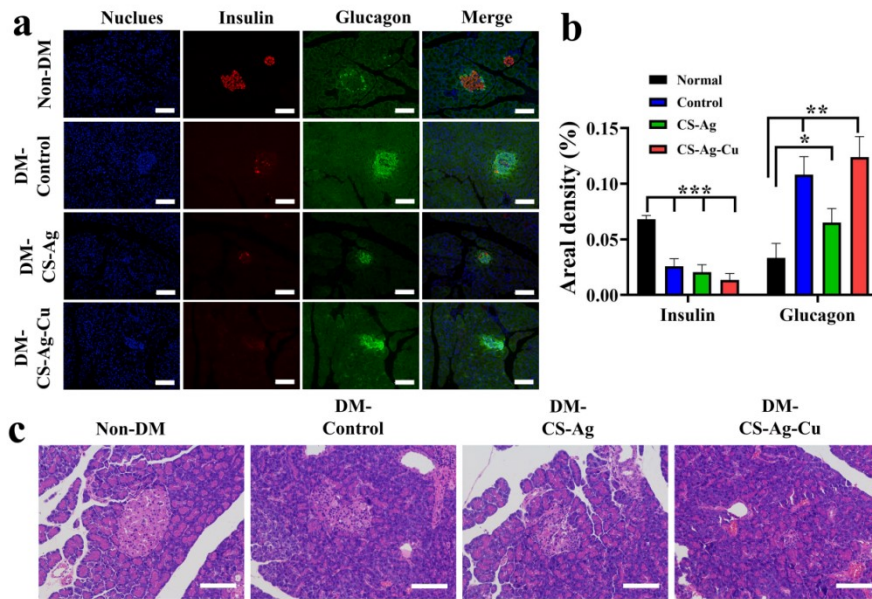


Fig. S14. (a) Immunofluorescence staining images of pancreas from different groups (Scale bar = 100 μ m). (b) Quantitative analysis of the relative areal density of insulin and glucagon. (c) H&E staining images of pancreas from different groups (Scale bar = 100 μ m). Data are expressed as mean \pm SD. ($n = 3$). * $p < 0.05$, ** $p < 0.01$, *** $p < 0.001$.

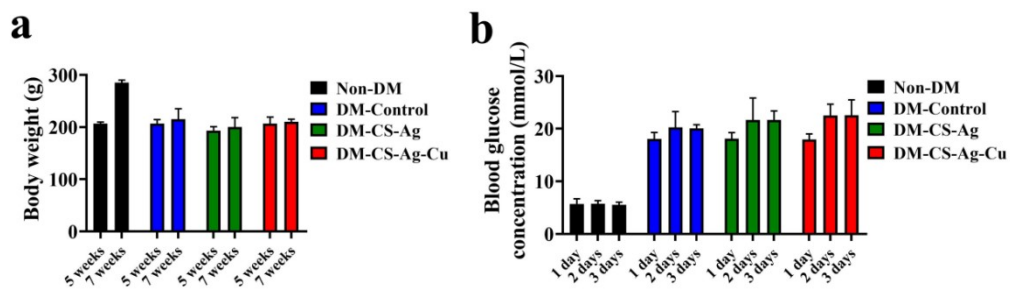


Fig. S15. (a, b) Body weights (a) and blood glucose levels (b) of rats in different groups were monitored after STZ injection. Data are expressed as mean \pm SD. ($n = 3$).

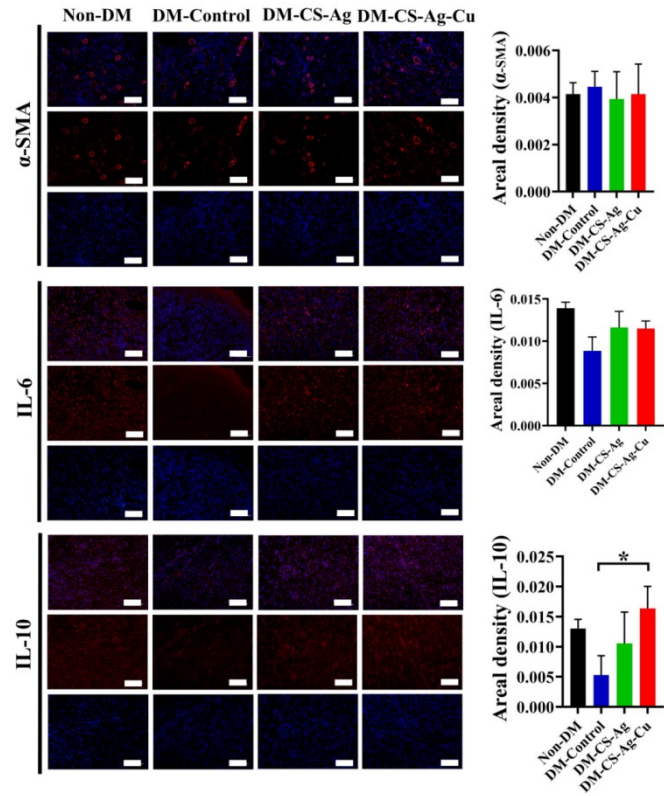


Fig. S16. Immunofluorescence staining of α -SMA/IL-6/IL-10 (red) and DAPI (blue) of skin wound tissues after 8 days of treatment and corresponding statistical data (Scale bar = 100 μ m). Data are expressed as mean \pm SD. ($n = 3$). * $p < 0.05$, ** $p < 0.01$, *** $p < 0.001$.

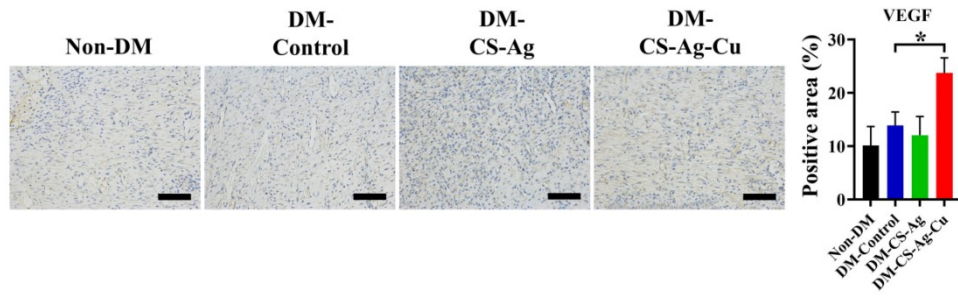


Fig. S17. Immunohistochemistry staining images of VEGF in wound tissues after 8 days of treatment and corresponding statistical data (Scale bar = 100 μ m). Data are expressed as mean \pm SD. ($n = 3$). * $p < 0.05$, ** $p < 0.01$, *** $p < 0.001$.

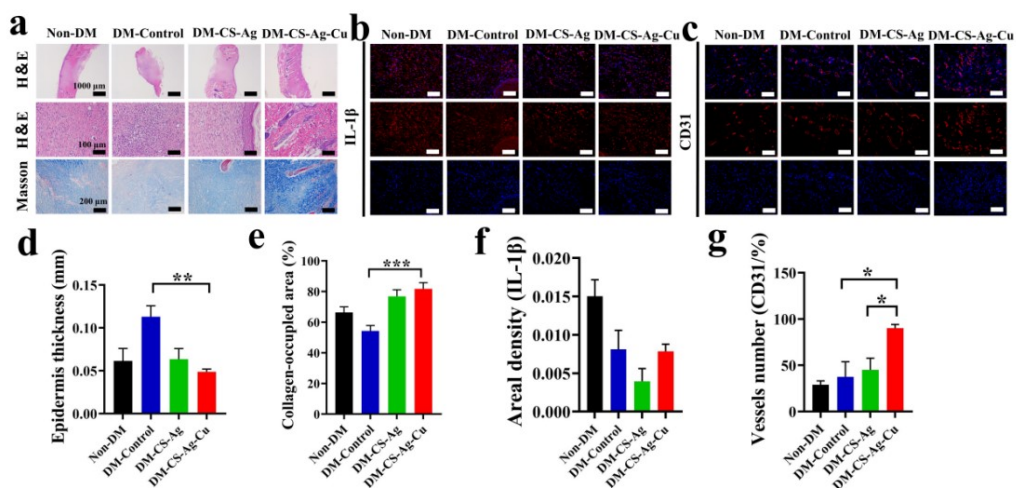


Fig. S18. Evaluation of diabetic skin wound repair after 14 days of treatment *in vivo*. (a) Micrographs of H&E and Masson staining tissue slices from different groups. (b, c) Immunofluorescence images of the expression of IL-1 β (b)/CD31 (c) (red) and DAPI (blue) in skin wound tissues on day 14 (Scale bar = 100 μ m). (d-g) Quantitative analysis of epidermis thickness (d), collagen deposition (e), areal density of IL-1 β (f) and vessels number (g) for each group. Data are expressed as mean \pm SD. ($n = 3$). * $p < 0.05$, ** $p < 0.01$, *** $p < 0.001$.

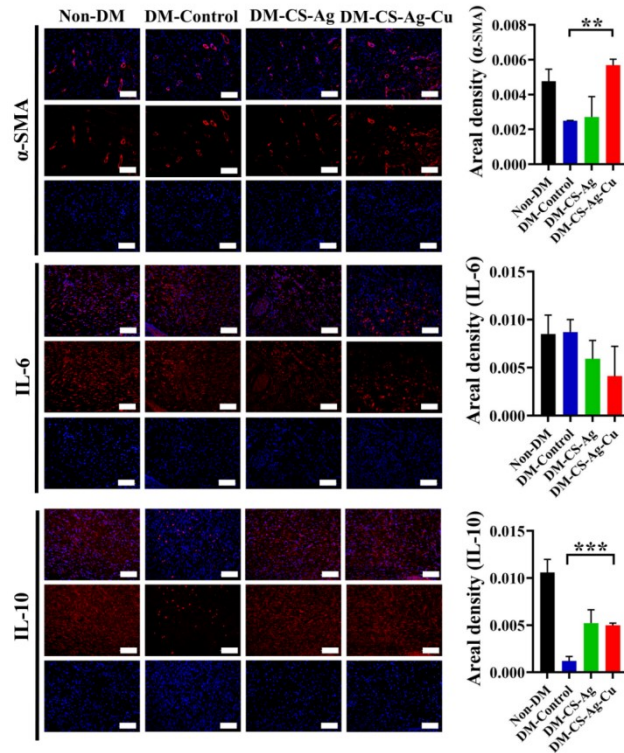


Fig. S19. Immunofluorescence staining images of α -SMA/IL-6/IL-10 (red) and DAPI (blue) of skin wound tissues after 14 days of treatment and corresponding statistical data (Scale bar = 100 μ m). Data are expressed as mean \pm SD. ($n = 3$). * $p < 0.05$, ** $p < 0.01$, *** $p < 0.001$.

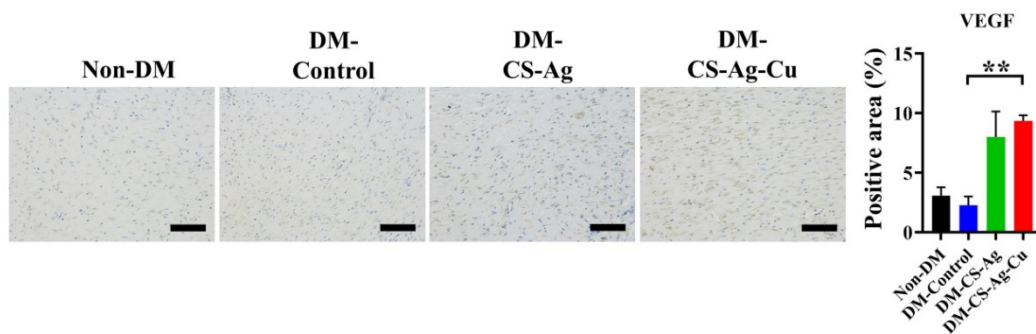


Fig. S20. Immunohistochemistry staining images of VEGF in wound tissues after 14 days of treatment and corresponding statistical data (Scale bar = 100 μ m). Data are expressed as mean \pm SD. ($n = 3$). * $p < 0.05$, ** $p < 0.01$, *** $p < 0.001$.

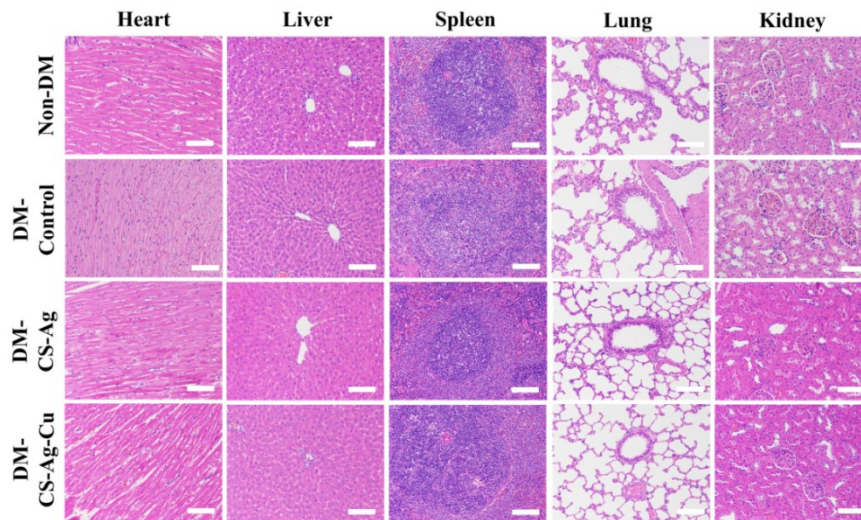


Fig. S21. H&E staining images of heart, liver, spleen, lung and kidney tissue slices in diabetic rats (Scale bar = 100 μ m).

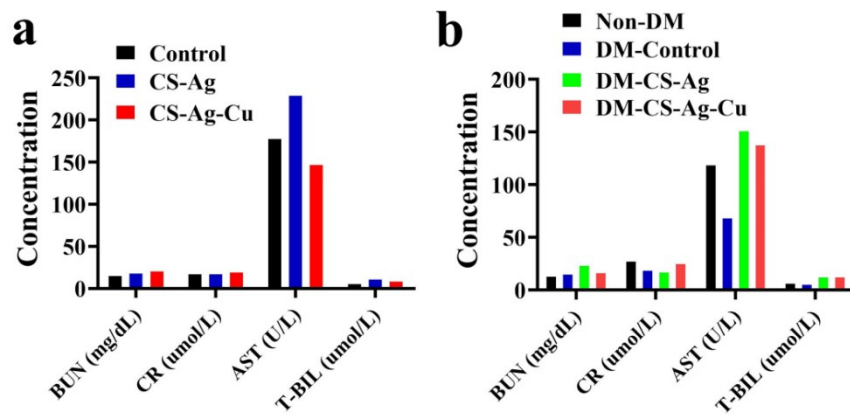


Fig. S22. (a, b) Blood biochemical tests in *S. aureus* infected (a) and diabetic (b) rats after 14 days of treatment.

Table S1. Blood routine analysis of *S. aureus* infected wound rats.

	Normal Range	Control	CS-Ag	CS-Ag-Cu
WBC	2.9-15.3 (10 ⁹ /L)	17.6	14.8	8.7
Lymph	2.6-13.5 (10 ⁹ /L)	12.6	8.6	5.4
Mon	0.0-0.5 (10 ⁹ /L)	0.5	1.5	0.3
Gran	0.4-3.2 (10 ⁹ /L)	4.5	4.7	3.0
Lymp %	63.7-90.1 (%)	71.3	57.7	62.4
Mon %	1.5-4.5 (%)	3.0	10.3	3.5
Gran %	7.3-30.1 (%)	25.7	32.0	34.1
RBC	5.60-7.89 (10 ¹² /L)	6.54	7.30	6.33
HGB	120-150 (g/L)	144	152	127
HCT	36.0-46.0 (%)	41.9	43.9	39.5
MCV	53.0-68.8 (fL)	64.2	60.2	62.5
MCH	16.0-23.1 (pg)	22.0	20.8	20.0
MCHC	300-341 (g/L)	343	346	321
RDW	11.0-15.5 (%)	11.1	12.5	12.5
PLT	100-1610 (10 ⁹ /L)	1457	1035	1124

Table S2. Blood routine analysis of diabetic rats.

	Normal Range	Non-DM	DM-Control	DM-CS-Ag	DM-CS-Ag-Cu
WBC	2.9-15.3 ($10^9/L$)	6.3	22.8	4.0	5.0
Lymph	2.6-13.5 ($10^9/L$)	4.5	15.3	2.5	3.5
Mon	0.0-0.5 ($10^9/L$)	0.2	0.8	0.1	0.2
Gran	0.4-3.2 ($10^9/L$)	1.6	6.7	1.4	1.3
Lymp %	63.7-90.1 (%)	72.1	66.8	61.8	70.6
Mon %	1.5-4.5 (%)	2.7	3.6	3.8	3.2
Gran %	7.3-30.1 (%)	25.2	29.6	34.4	26.2
RBC	5.60-7.89 ($10^{12}/L$)	6.96	7.88	6.72	7.63
HGB	120-150 (g/L)	124	151	118	148
HCT	36.0-46.0 (%)	38.6	43.6	37.5	44.5
MCV	53.0-68.8 (fL)	55.5	55.4	55.9	58.4
MCH	16.0-23.1 (pg)	17.8	19.1	17.5	19.3
MCHC	300-341 (g/L)	321	346	314	332
RDW	11.0-15.5 (%)	12.2	12.8	10.9	13.4
PLT	100-1610 ($10^9/L$)	138	812	582	1240